Materials Science & Engineering A 703 (2017) 37–44

Contents lists available at ScienceDirect

Materials Science & Engineering A

journal homepage: www.elsevier.com/locate/msea

New insights to damage initiation during creep deformation of stainless steel weld joints

V.D. Vijayanand*, V. Ganesan, K. Laha

Creep Studies Section, Metallurgy and Materials Group, Indira Gandhi Centre for Atomic Research, Kalpakkam 603102, India

ARTICLE INFO

Keywords:
Austenitic stainless steel
Weld joints
Multi-pass weld joint
Creep cavitation

ABSTRACT

A systematic investigation has been carried out to asses the creep cavitation behaviour in austenitic stainless steel fusion zone by performing detailed microstructural and finite element analysis. Metallographic observations of the failed cross-weld joint specimens reveal that the cavities nucleated in the near-crown region and propagated towards the near-root region. Similar pattern of nucleation and growth of cavities was observed in weld joint tested at a different stress level. The preferential nucleation of creep cavities in the near-crown region of the weld joint can be attributed to both micro and macro inhomogeneities in the weld joint. The micro-inhomogeneity in the fusion zone, which could be characterized using electron backscatter diffraction studies, is a result of variations in morphology and formation of thermo-mechanically treated region across the weld pass interface. The considerable strength variation between the heat affected zone, base metal and fusion zone resulted in macro-inhomogeneity in the weld joint and introduced significant stress gradients which could be illustrated using finite element analysis. Both micro and macro-inhomogeneities have a synergistic role in determining the damage initiation location in multi-pass stainless steel weld joints subjected to creep.

1. Introduction

Austenitic stainless steel is the prime structural material used for fabricating fast breeder reactor's structural components [1]. This material is a unanimous choice as it exhibits superior creep strength, adequate hot corrosion resistance and has good compatibility with liquid sodium [2]. As welding is the most widely resorted technique for fabricating huge components of the reactor, evaluating the creep strength of the weld joints is also as crucial as assessing the creep properties of the base material. Creep strength of a material is usually evaluated based on its ability to resist high temperature deformation as well as microstructural damage. Both deformation and microstructural damage influence the rupture life of the material. As components in nuclear reactors operate well within the allowable design stress limits, it is the time dependent damage in the material which is the predominant life limiting factor. Creep damage in austenitic stainless steel is usually attributed to nucleation and growth of cavities [3]. Creep cavitation reduces the effective load bearing capability of the component, which may in turn result in dimensional intolerance due to the consequent localised deformation. Elaborate assessment of the creep damage which results due to cavitation in the fusion zone, can offer new perspectives for any possible microstructural and design modifications. This in turn can help mitigate the influence of cavitation induced damage on the failure of welded austenitic stainless steel components.

In case of the austenitic stainless steel base metal, cavities during creep exposure usually initiate as a result of interactions between the grain boundary sliding phenomenon and chromium carbide precipitates [3]. For shorter durations of creep exposure when the carbides are finer in size, they pin grain boundaries effectively which obstructs sliding. Prolonged elevated temperature exposure results in significant coarsening of the carbides which render them as inefficient barriers for grain boundary sliding. This results in considerable grain boundary sliding resulting in nucleation of cavities at either triple points or at the chromium carbide precipitate interface [4].

In case of the fusion zone, regions containing delta ferrite exhibit creep cavitation [5]. A certain amount of delta ferrite is intentionally prescribed in austenitic steel fusion zone to prevent hot cracking [6]. The grain size in the fusion zone is coarser than the base metal [7] and has higher grain boundary facet length making the microstructure more susceptible to cavitation. As delta ferrite phase is a metastable phase with a relatively open body-centred cubic crystal structure when compared to the close packed face-centred cubic structure of austenite, it readily transforms into brittle intermetallic phases like sigma, chi, Laves. These transformations in addition to the precipitation of chromium carbide occur at shorter time durations when compared to the

* Corresponding author.
E-mail address: vdvijayanand@igcar.gov.in (V.D. Vijayanand).

http://dx.doi.org/10.1016/j.msea.2017.07.057
Received 1 June 2017; Received in revised form 17 July 2017; Accepted 18 July 2017
Available online 19 July 2017

transformations occurring in the close-packed austenite phase. As the intermetallics and precipitates coarsen, their role in resisting grain boundary sliding diminishes gradually, resulting in nucleation of cavities at the interface [8]. Further, the presence of coarser grain size in the fusion zone results in higher facet length, which reduces the threshold stress required for cavity nucleation [9].

Thus it can be stated that in case of fusion zone the transformation of delta ferrite and in case of base metal the coarsening of carbides are the crucial phenomena which influence creep cavitation in each of these respective regions. It should be noted here that in a composite austenitic stainless steel weld joint which consists of base metal and fusion zone, the precipitation of intermetallic phases and chromium carbides from delta ferrite in the fusion zone occurs more rapidly at elevated temperature exposures when compared to the precipitation and subsequent coarsening of carbides in the austenitic base metal [10]. This results in an earlier onset of creep cavitation in the fusion zone when compared to the base metal region of the weld joint. Therefore, studies pertaining to damage evolution in the fusion zone of stainless steel are more essential for assessing the performance of the welded components.

Unlike the base metal, microstructure of the fusion zone is highly heterogeneous, which makes studies on creep cavity nucleation more complicated. The primary source for the formation of heterogeneities is the laying of multiple passes and the associated thermal cycling which modifies the microstructure of the weld metal which is deposited by preceding passes. It has been reported that two distinct modifications occur in the weld metal due to the deposition of the subsequent pass. One of the modifications is associated with change of delta ferrite morphology and the other is with respect to the formation of an intrinsic thermo-mechanically strengthened region [11,12]. Studies on shielded metal arc welding (SMAW) joints have shown that deposition of subsequent pass modifies the structure of delta ferrite from vermicular to globular [11]. In order to comprehensively understand the prevalence of a thermo-mechanically region, investigations were undertaken on dual pass activated tungsten inert gas (A-TIG) welded joint. As A-TIG is an autogenous welding process, the influence of delta ferrite and its morphological changes was minimised. Using impression creep testing it was shown that the strength of the first laid pass was significantly higher than that of the pass which was laid subsequently. This study clearly established that the deposition of subsequent passes strengthen the previously deposited weld layers [13].

Cavitation in the fusion zone can be linked to the nature and distribution of the inhomogeneities. In this study, a thorough investigation is undertaken to evaluate the influence of various types of inhomogeneities on creep cavitation. Based on these results the possible reasons for creep cavitation to initiate at certain specific regions of the fusion zone have been critically examined.

2. Experimental

The chemical composition of the base material and electrode is given in Table 1. The details of the SMAW parameters are furnished in Table 2. The groove angle in the base plate was 10°. The weld joint specimen was composed of the three constituents the fusion zone in the central region, flanked by the HAZ as well as the base metal regions. A schematic of the specimen is given in Fig. 1. Uniaxial creep tests were carried out at stress levels of 140 and 200 MPa at 923 K. Automated ball indentation (ABI) testing was carried out using a spherical indenter of 0.76 mm diameter. The indentor and was made of silicon carbide. ABI tests were performed at a temperature of 923 K and speed of the cross head was maintained at 0.008 mm s^{-1}. Impression creep (IC) tests were carried out at 923 K using a flat bottomed cylindrical indenter of 1 mm diameter. For metallographic analysis, the weld joint specimens were polished by standard metallographic procedure up to a surface finish of 1 µm. These specimens were subsequently electrolytically etched using a solution containing 60% HNO_3 and 40% H_20 solution at 2 V for 30 s before observation. Micro-hardness measurements were taken using Vickers hardness tester employing a load of 200 gf. Specimens for electron back scatter diffraction (EBSD) were electro-polished before observation. EBSD data was acquired using Carl Zeiss Supra 55 FEG-SEM. The FEG was subjected an acceleration voltage of 20 kV. The specimen was placed in a 70° pre-tilted holder with a working distance of 16 mm. The distribution of low and high angle grain boundaries was characterized using HKL-Channel 5 software. Finite element analysis was carried out using ABAQUS version 6.11 finite element solver. The four-node three dimensional linear tetrahedron element (C3D4) was used for meshing the geometry. The mesh size was refined until convergent values for the stress values were obtained.

Table 1
Chemical composition range of 316LN SS base metal and 316(N) electrode in wt%.

	C	Ni	Cr	Mo	Mn	Si	S	P	N
316 LN SS base metal	0.025	12.15	17.57	2.53	1.74	0.2	0.004	0.017	0.14
316 (N) SS weld metal	0.051	11.2	18.45	1.94	1.37	0.48	0.005	0.024	0.13

Table 2
Welding parameters.

Electrode size (mm)	4
Current (A)	128
Voltage (V)	24
Travel speed (mm/min)	97
Heat input (kJ/mm)	1.89 (each pass)

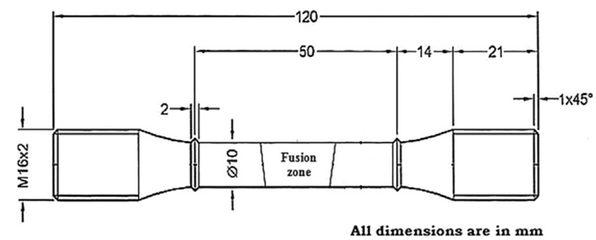

Fig. 1. Schematic of weld joint specimen.

3. Results and discussions

3.1. As-received microstructure

The macrostructure of the weld joint is the as-welded condition is shown in Fig. 2. It can be seen from the figure that the fusion zone is composed of several layers. The fusion zone consisted of dendritic austenite grains with 3–5 vol% delta ferrite. Fig. 3(**a and b**) show the hardness variation across the X-X′ (base metal-HAZ-fusion zone-HAZ-base metal) and Y-Y′ (crown to root region of the fusion zone) lines indicated in Fig. 2. It can be seen that the hardness in the fusion zone and heat affected zone are substantially higher when compared to the base metal. The fusion zone is hardened due to the restraint imposed by the adjoining base metal and the solidification stresses which causes considerable increase in dislocation density in this dendritic microstructure [14]. It has been reported that the dislocation structure in the fusion zone of stainless steel can be compared to that of the heavily cold worked structures [15]. The HAZ in stainless steel weld joints is hardened due to the repeated thermal cycling generated during the multipass welding [16]. The increase in hardness from the crown to root region (Y-Y′) indicates that the root region is significantly hardened due to the deposition of subsequent passes. The dashed lines in Fig. 2